COBEM 2021 26th International Congress of Mechanical Engineering
ABCM Associação Brasileira de Engenharia e Ciências Mecânicas
November 22-26, 2021, Virtual Congress, Brazil

COBEM2021-0814
NUMERICAL ANALYSIS OF THIN FILM EVAPORATION A STUDY ABOUT CELLS CRYOPRESERVATION

Guilherme Dahmer Steffenon
Jacqueline Biancon Copetti
Mario Henrique Macagnan
Alisson Renan Stochero da Silva
Massoxi Mandela Cuieca
University of Vale do Rio dos Sinos, Mechanical Engineering Graduate Program, LETEF, Laboratory of Thermal and Fluid Dynamic Studies, Unisinos Avenue, 950, São Leopoldo, 93022-750, RS, Brasil.
guilhermesteffenon@gmail.com, jcopetti@unisinos.br, mhmac@unisinos.br, alissonstochero@hotmail.com, massoxymandela@hotmail.com.

Jeferson Diehl de Oliveira
FSG - University Center, Center of Innovation and Technology, Department of Mechanical Engineering, Os Dezoito do Forte, 2366, Caxias do Sul, 95020-472, RS, Brazil,e-mail: jeferson.physics@gmail.com

Abstract. *Cryopreservation is a prominent area that studies the different ways of cell preservation for future use. In this work, the cryopreservation process using thin film evaporation method was analyzed. The evaporation of liquid nitrogen, the water solidification process, and the temperature distribution in the studied domain over time were evaluated. This analysis was performed using a numerical model (CFD) in ANSYS Fluent ® software to simulate the solidification process by thin film evaporation, showing the viability of this technique to the cryopreservation of cells. In addition, the work can determine a cooling rate of about 120,000°C/min and a total sample solidification time of 0.027 seconds.*

Keywords: *Thin Film Evaporation, Cryopreservation, CFD, Numerical Simulation.*

1. INTRODUCTION

Biopreservation is an area of research known for encompassing processes that suppress biological aging while using preservation processes, which aim at further restoration of cellular functions after preservation. This area is also known as cryopreservation, since to carry out these processes it is necessary to use cryogenic temperatures. Cryopreservation incorporates important engineering principles that are relevant to cellular and molecular development, always aiming to keep cells alive and healthy for future uses (Baust *et al.*, 2009).

This conservation process is carried out by cooling at low temperatures, where ovaries, embryos, sperm and other tissues are preserved. In the case of human embryos and sperm, there are several recognized protocols for their cryopreservation, which is classified as a slow cooling process (Shaw and Jones, 2003).

Cryopreservation is basically a technology used to preserve cells, maintaining their viability and their functions at temperatures ranging from -80°C to -196°C. This cell freezing process can occur quickly (vitrification) or slowly (slow freezing), where the use of cryoprotective agents (CPAs) is necessary. Cryoprotectors are important because they reduce possible cryoinjuries caused by the formation of ice crystals in cells, in addition to increasing the efficiency of cell conservation (Yang *et al.*, 2019).

In relation to vitrification and slow freezing, its main difference is in relation to the cooling rate and the use of CPAs. Slow freezing has low freezing rates ranging from 10 °C/min to 100 °C/min and uses low concentrations of CPAs (about 1~2 mol/l). On the other hand, vitrification presents high rates starting from 10.000 °C/min up to the maximum that the method used allows, in addition to requiring a higher concentration of CPAs compared to slow freezing (Shaw and Jones, 2003).

Vitrification is a widely studied alternative where it usually uses liquid nitrogen to remove heat from the cells through a sudden evaporation. As a result of this process the temperature of cell samples rapidly reduces to -196°C, which represents the temperature of liquid nitrogen at atmospheric pressure. This suddenly reduction of temperature avoids the formation of ice crystals in the temperature of solidification. Among the various processes that carry out vitrification, the one with greater flexibility and cooling rates greater than 40,000 °C/min is the thin film evaporation process (Su *et al.*, 2017).

In view of this recent use of thin film evaporation as an alternative to cryopreservation processes, this process will be analyzed numerically in the present work in order to be able to evaluate the ideal conditions of the method in the future.

2. THIN FILM EVAPORATION

Evaporation is a process of heat transfer and phase change that takes place at the interface between liquid and vapor. This occurs when the pressure is less than the liquid saturation pressure for a given temperature.

Usually in different processes, such as pool boiling, the formation of a layer of vapor occurs, known as "vapor blanket", which acts as an unwanted thermal insulator and limits the heat transfer coefficient between the surface and the liquid nitrogen. With the evaporation process, when used in liquid nitrogen freezing processes, the fluid is injected into the sample in order to avoid the formation of this "vapor blanket". Thus, it was realized that the use of a thin film evaporation process that flows through the surface would enable an increase in heat transfer, further increasing the cooling rate (Su *et al.*, 2017).

According to Plawsky *et al.* (2014), thin film evaporation is a process divided into 3 flow regions. Each of these regions has some characteristics, as shown in Figure 1.

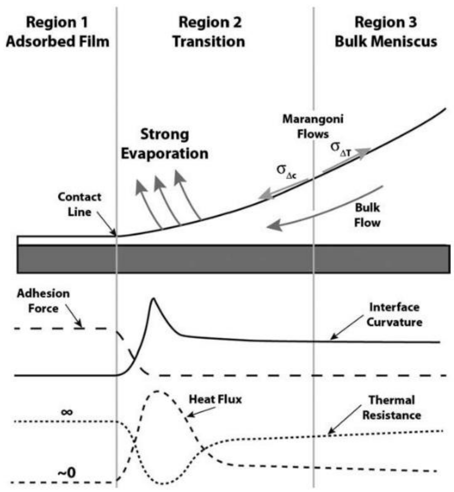

Figure 1. Variation in adhesion force, curvature, heat flux and thermal resistance in the contact line region for an evaporating meniscus (Plawsky *et al.*, 2014).

In the regions presented by Plawsky *et al.* (2014), we can highlight the transition region where it presents the point with the highest heat transfer due to lower thermal resistance and adhesion forces. This region is where it is possible to optimize the evaporation process, making it occur with the best possible efficiency. Thin film evaporation is an important heat transfer process through phase change, where the fluid flow mechanism and the evaporation of the film ensure an increase in the convective heat transfer coefficient (Demsky and Ma, 2004).

In a work by Su *et al.* (2017) a way to carry out the thin film evaporation process for cell cryopreservation was presented. The process was constructed so that liquid nitrogen encountered the external surface of the evaporator that contained the samples. Figure 2 shows the scheme of how the equipment was builded in the laboratory by the researchers.

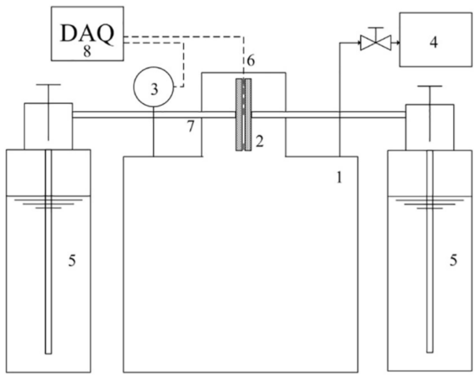

Figure 2. Schematic of experimental system (1. Vacuum chamber, 2. Frozen carrier, 3. Pressure sensor, 4. Vacuum pump, 5. Liquid nitrogen container, 6. Thermocouples, 7. Liquid nitrogen jet tubes and 8. Data acquisition system.) (Su *et al.*, 2017)

In the system, the liquid nitrogen basically flows until it encounters the evaporator in the form of jets that spread along its surface. With this, a thin film is generated on the two surfaces of the evaporator, thus freezing the sample down to a temperature of -196°C. The sample used in the experiments was an aqueous solution of DMSO (Dimethyl Sulfoxide).

It should be noted that the evaporator is basically made up of two copper plates that have finned surfaces on the outside that favor heat transfer. The evaporator design used in some of the authors' tests is shown in Figure 3.

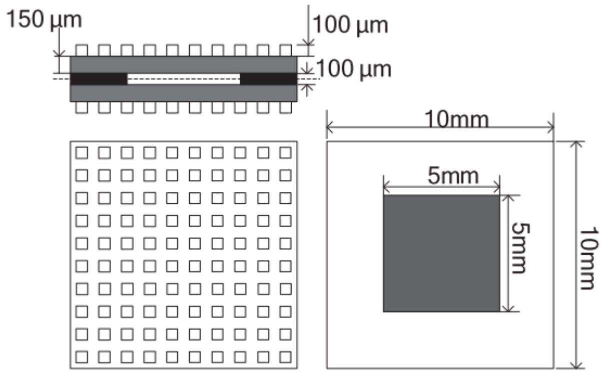

Figure 3. Frozen carrier diagram (Su *et al.*, 2017)

Given the importance of this method that allows achieving high freezing rates, this work aims to perform a numerical analysis of the experiment through modeling via CFD according to the conditions of the experiment.

3. MATERIALS AND METHODS

In this work, numerical simulation (CFD) of thin-film evaporation was carried out based on the working conditions mentioned in the work by Su *et al*. (2017), where the sample considered was water. In the simulations it is possible to analyze the liquid nitrogen flow, the nitrogen evaporation, the water solidification and the cooling rate.

3.1 Geometry

Initially, the geometry that would represent the domain used for the simulations was developed. In Figure 4 it is possible to identify the left side of the evaporator (Figure 2, point 7), that is, half of the system used in the laboratory. In the simulations, the dimensions of the finned evaporator were reproduced as shown in Figure 3, with the square fins of 100 µm x 100 µm and the distance between them of 100 µm.

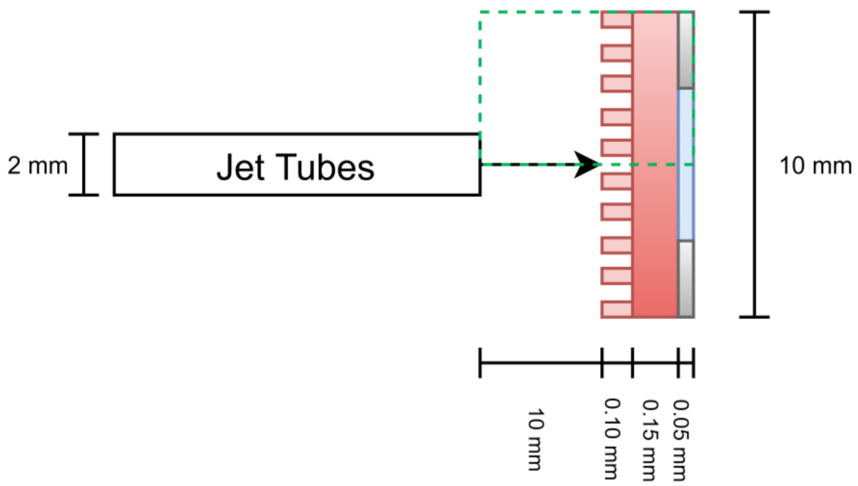

Figure 4 – Left side of evaporator dimensions

As the geometry continues to show symmetry in the vertical direction, the domain used for the simulations was reduced to represent the dotted green area of the Figure 4. In addition, a two-dimensional domain was considered, starting from the output of the liquid nitrogen jet to the section of added water inside the evaporator, as shown in Figure 5.

Figure 5 – 2D Geometry used in simulation

3.2 Mesh

To create the mesh of the problem, two sizes of elements were considered, making the elements in the regions closest to the evaporator to present the greatest refinement and the greatest efficiency in demonstrating the phenomena that occur at the site. The sizes used for the elements were 0.05 mm and 0.01 mm using the MultiZone Quad method and considering all quadrilateral elements.

The mesh used can be seen in Figure 6, where it is possible to see the change in the size of elements between regions.

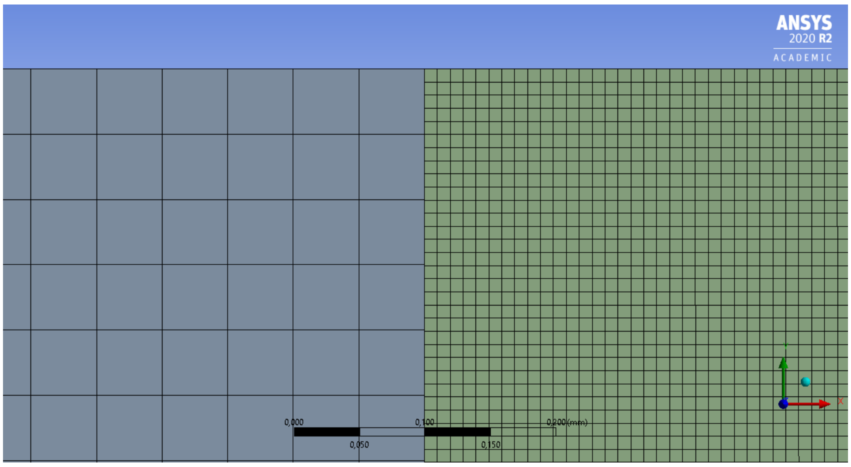

Figure 6 – Mesh used in the simulation

A mesh convergence study using the GCI Method (Celik et al., 2008) was used, using 3 meshes with a refinement factor between 1.4 and 1.5. The meshes used had a total of 393555, 193327 and 86002 elements, using the point temperature (0,0,0) as the control variable. After the convergence analysis, a convergence index of 1.27% was detected for meshes 1 and 2, making mesh 2 can be used to simulate the phenomena.

3.3 Setup and Equations

The setup used in the numerical simulations for thin film evaporation was performed using the VOF (Volume of Fluid), Solidification and Energy models present in ANSYS Fluent ®. The process was simulated considering a transient formulation lasting about 0.1 s, with a time step of 0.001s size and with a viscosity model defined as turbulent (k-epsilon).

The ANSYS Fluent ® software basically used the following equations to perform the calculations. Initially, the energy equation adapted for the VOF, represented in Eq. 1, was used.

$$\frac{\partial}{\partial t}(\rho E) + \nabla \cdot \big(\vec{v}(\rho E + p)\big) = \nabla \cdot \big(k_{eff}\nabla T - \textstyle\sum_q \sum_j h_{j,q}\vec{J}_{j,q} + (\bar{\bar{\tau}}_{eff} \cdot \vec{v})\big), \quad (1)$$

where ρ is the density, E is the energy, $\vec{v}$ is the velocity, p is the pressure, k_{eff} is the effective thermal conductivity, ∇T is the temperature gradient, $h_{j,q}$ is the enthalpy of the species *j* in phase *q*, $\vec{J}_{j,q}$ is the diffusive flux of species *j* in phase *q* and $\bar{\bar{\tau}}_{eff}$ is the effective time constant.

For the continuity equation, the General Equation of the VOF model, represented in Eq. 2, was used. In the program, an implicit formulation for the VOF model was also considered.

$$\frac{1}{\rho_q}\left[\frac{\partial}{\partial t}\left(\alpha_q\rho_q\right) + \nabla\cdot\left(\alpha_q\rho_q\overrightarrow{v_q}\right) = \sum_{p=1}^{n}(\dot{m}_{pq} - \dot{m}_{qp})\right], \quad (2)$$

where ρ_q is the density of the *q* phase, α_q is the volume fraction of the *q* phase, $\overrightarrow{v_q}$ is the velocity of the *q* phase, $\dot{m}_{pq}$ is the mass flow rate from the *p* phase to the *q* phase and $\dot{m}_{qp}$ is the mass flow rate of the *q* phase to *p* phase.

Subsequently, the software applied the moment equation adapted for VOF and the Lee equation for evaporation, which considers the evaporation of nitrogen, being represented by Eq. 3 and Eq. 4, respectively.

$$\frac{\partial}{\partial t}(\rho\vec{v}) + \nabla\cdot(\rho\vec{v}\vec{v}) = -\nabla_p + \nabla\cdot[\mu(\nabla\vec{v} + \nabla\vec{v}^T)] + \rho\vec{g} + \vec{F}\,, \quad (3)$$

where ρ is the density, $\vec{v}$ is the velocity, μ is the dinamic viscosity, $\vec{g}$ is the gravity acceleration and $\vec{F}$ is a force applied in the process.

$$\frac{\partial}{\partial t}(\alpha_v\rho_v) + \nabla\cdot\left(\alpha_v\rho_v\vec{V}_v\right) = \dot{m}_{lv} - \dot{m}_{vl}\,, \quad (4)$$

where α_v is the volume fraction of vapor, ρ_v is the density of vapor, $\vec{V}_v$ is the velocity of the vapor, $\dot{m}_{lv}$ and $\dot{m}_{vl}$ are the mass flow rate for evaporation and condensation, respectively.

Finally, the equations relating the solidification process that occurs with water, represented by Eq. 5 and Eq. 6.

$$S = \frac{(1-\beta)^2}{(\beta^3+\varepsilon)}A_{mush}(\vec{v} - \vec{v}_p)\,, \quad (5)$$

where S is the source term, β is the volumetric fraction of liquid, ε is a small number to avoid divisions by zero, A_{mush} is the mush zone constant, $\vec{v}_p$ is the traction velocity of the solid.

$$\begin{aligned} &\beta = 0 \ if\ T < T_{solidus}, \\ &\beta = 1 \ if\ T > T_{liquidus}, \\ &\beta = \frac{T - T_{solidus}}{T_{liquidus} - T_{solidus}} \ if\ T_{solidus} < T < T_{liquidus}\,, \end{aligned} \quad (6)$$

where T is the temperature, $T_{solidus}$ is the solid temperature and $T_{liquidus}$ is the liquid temperature.

4. RESULTS AND DISCUSSION

To carry out the simulations, it was necessary to determine a pressure difference that would guarantee the flow of liquid nitrogen to the evaporator. Therefore, a liquid nitrogen inlet pressure of 101.325 kPa and a chamber pressure of 10.30 kPa were considered.

The results were treated through the CFD Post software present in the ANSYS system, where it was possible to collect values and images of how the process occurred.

4.1 Flow Nitrogen Profile

The first analyzed result obtained was the volume fraction of liquid nitrogen profile during the thin film evaporation process. It is possible to visualize in Figure 7 the flow profile of liquid nitrogen in the first 0.05 s. It is worth noting that the behavior remained constant after 0.05 s, with only a variation over time in the formation of vapor on the finned surface.

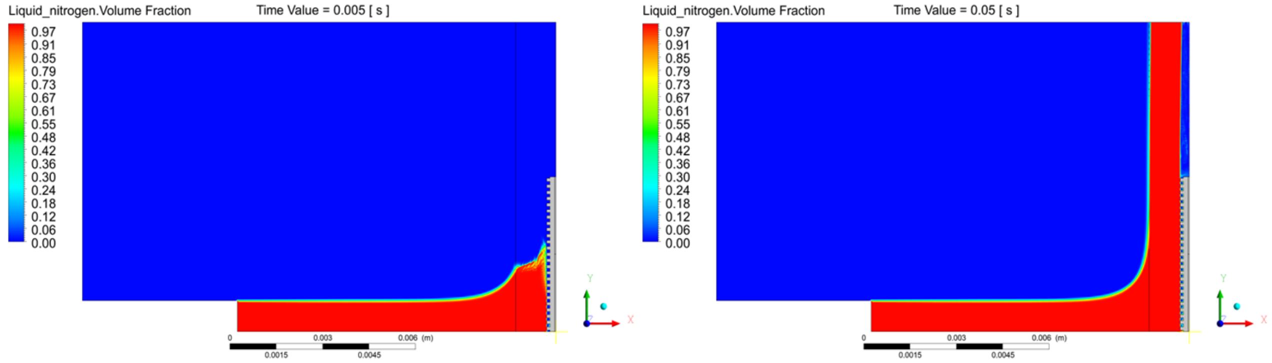

Figure 7 – Contour of the volume fraction of liquid nitrogen in the domain at different times

4.2 Temperature profile

As with the nitrogen flow profile, it is possible to evaluate the temperature distribution profile over time. Figure 8 shows this process, it is worth noting that after 0.1s the entire evaporator system (fins and water) is at a equilibrium temperature with liquid nitrogen.

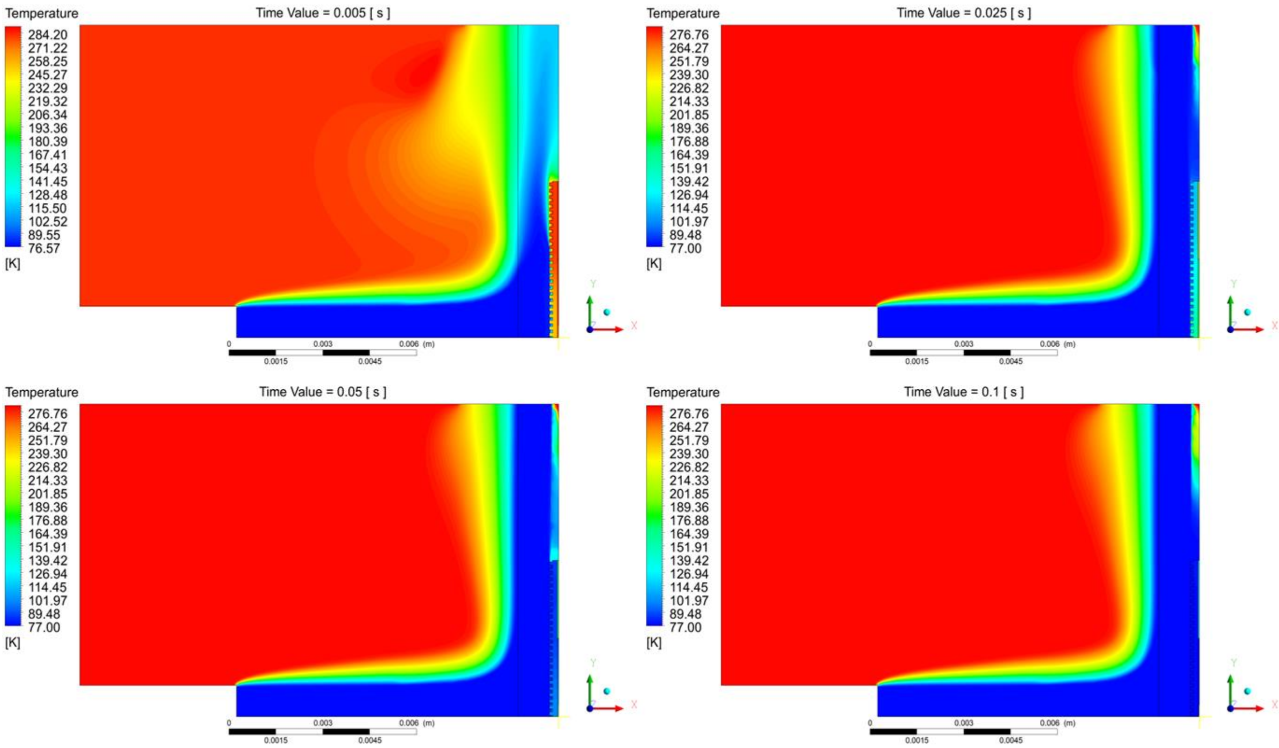

Figure 8 – Contour of the temperature in the domain at different times

As we can see in the figure, the chamber temperature quickly stabilizes at -196°C around 0.025s. The rest of the process basically consists of heat transfer by conduction of the fins to the sample, which lasts another 0.075s.

In addition to the temperature distribution across the domain, the temperature over time at the point located at the 0 position of the X, Y, Z axes was also analyzed. This point would represent the center point of the water that is located inside the evaporator, such as we visualized in Figure 9. With this information, it is possible to determine that the water temperature has entered equilibrium with liquid nitrogen after 0.1 s.

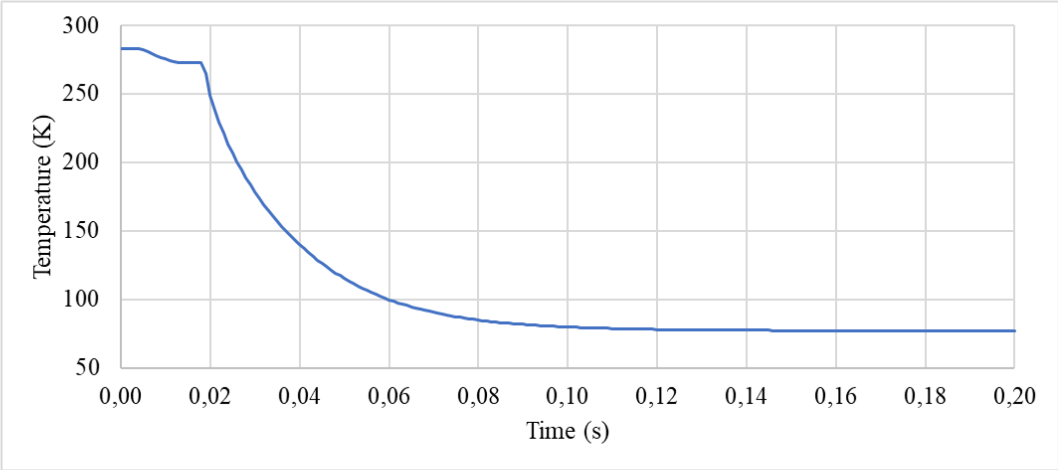

Figure 9 – Temperature of water in the center of the evaporator x Time

With this graph it is possible to determine the cooling rate of the process that was simulated, considering the temperature reduction from 10°C to -196°C in 0.12s. This generates a rate of approximately 103,000 °C/min, which demonstrates that the process has a high efficiency and makes it increasingly viable for use in cryopreservation processes.

4.3 Water Solidification and Nitrogen Evaporation

In the same way as the profiles analyzed above, it is possible to visualize the solidification of the water. At the time 0.015 s shown in Figure 10, we can see the solidification of water on the right side of the fins and the evaporation of liquid nitrogen on the left side of the fins.

This is interesting to analyze because it is possible to notice the formation of a nitrogen vapor film throughout the process, ensuring greater efficiency in heat transfer, considering that phase changes generate a higher heat flux.

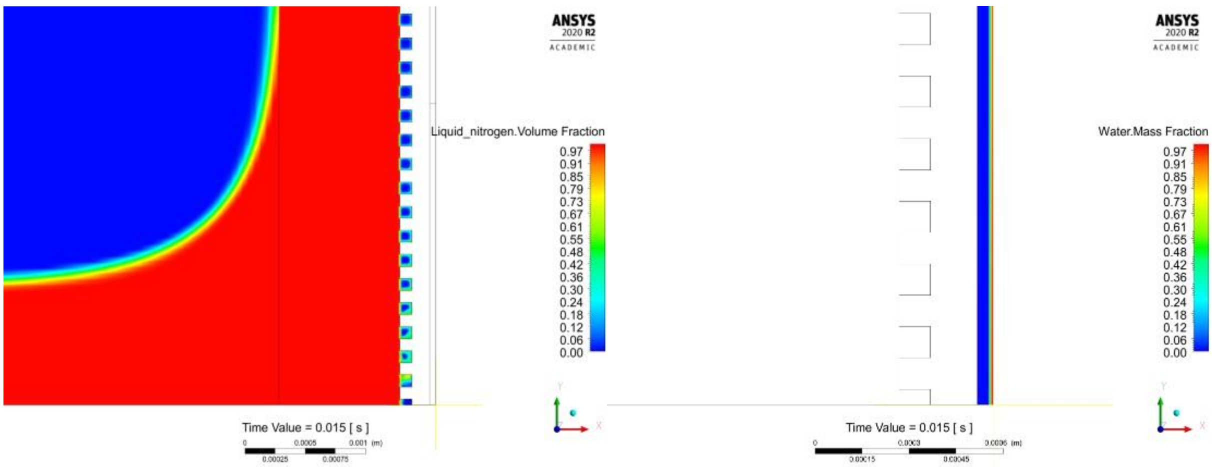

Figure 10 –Nitrogen evaporation and Water mass fraction variation during solidification

Finally, it is also important to check whether the water solidification process took place. In this case, a calculation of the average water mass fraction over time in the region where the water was located was performed. In Figure 11 this is represented over time, where it is possible to determine that in approximately 0.018s the water is fully solidified.

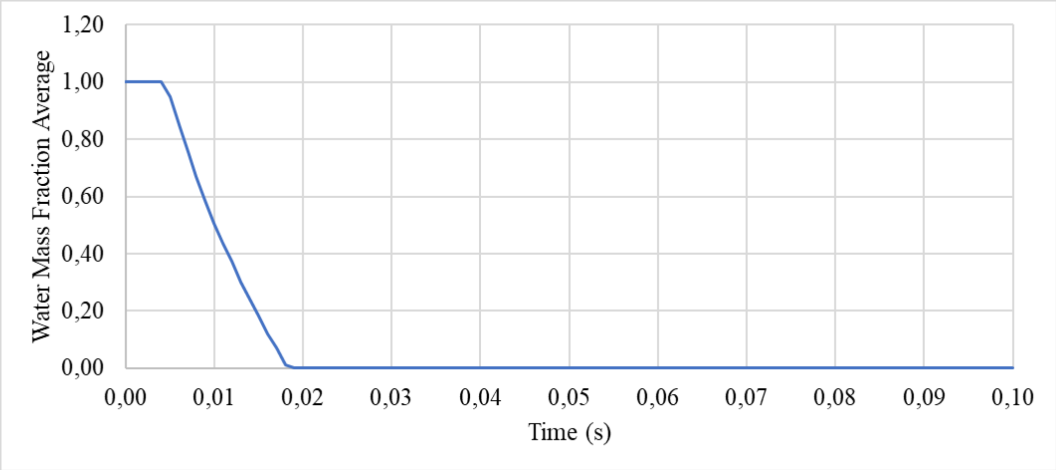

Figure 11 – Water mass fraction average of the evaporator x Time

5. CONCLUSION

With the simulations performed, it was possible to visualize the processes that occur in the thin film evaporation cryopreservation method, in addition to determining that:

- In the simulation, the cooling rate obtained was about 100,000°C/min;
- The solidification process was completed in 0.018s for the simulated conditions;
- It is possible to make changes in geometry and conditions to evaluate alternatives, always aiming to increase the cooling rate of the process.

6. REFERENCES

ANSYS Fluent ® Theory Guide 15.0, ANSYS, Inc. Canonsburg, PA (2013).

Baust, J.G., Gao, D., Baust, J.M., 2009. "Cryopreservation: An emerging paradigm change". *Organogenesis*. Vol.5, No. 3, pp. 90-6.

Celik, I.B., Ghia, U., Roache, P.J., Freitas, C.J., Coleman, H., Raad, P.E, 2008. "Procedure for Estimation and Reporting of Uncertainty Due to Discretization in CFD Applications." ASME. J. Fluids Eng. 130(7): 078001.

Demsky, S., Ma, H. B., 2004. "Thin Film Evaporation on a Curved Surface". *Microscale Thermophysical Engineering*, Vol.8, pp.285–299.

Plawsky, J.L., Fedorov, A.G., Garimella, S.V., Ma, H.B., Maroo, S.C., Chen, L., Nam, Y, 2014. "Nano and microstructures for thin-film evaporation – A review". *Nanoscale and Microscale Thermophysical Engineering*. Vol. 18, pp. 251–269.

Shaw, J.M., Jones, G.M., 2003. "Terminology associated with vitrification and other cryopreservation procedures for oocytes and embryos". *Human Reproduction Update*. Vol. 9, pp.583–605.

Su, F., Xu, H., Zhao, N., Deng, Y., Ma, H., 2017. "Evaporation heat transfer of liquid nitrogen on microstructured surface at high superheat level". *International Communications in Heat and Mass Transfer*. Vol. 87, pp. 192-197.

Yang, J., Gao, L., Liu, M., Sui, X., Zhu, Y, Wen, C., Zhang, L., 2020. "Advanced Biotechnology for Cell Cryopreservation". *Transactions of Tianjin Univesity*. Vol.26, pp. 409–423.

7. RESPONSIBILITY NOTICE

The authors are the only responsible for the printed material included in this paper.